



A label-free G-quadruplex DNA-based fluorescence method for highly sensitive, direct detection of cisplatin



Hualin Yang^a, Hanli Cui^a, Longgang Wang^a, Li Yan^a, Yong Qian^a, Xi Emily Zheng^a, Wei Wei^{a,b,*}, Jing Zhao^{a,b,*}

^a State Key Laboratory of Pharmaceutical Biotechnology, Institute of Chemistry and BioMedical Sciences, School of Life Sciences, Nanjing University, Nanjing 210093, China

^b Shenzhen Key Lab of Nano-Micro Material Research, Key Laboratory of Chemical Genomics, Shenzhen Graduate School of Peking University, Shenzhen 518055, China

ARTICLE INFO

Article history:

Received 24 January 2014

Received in revised form 26 February 2014

Accepted 9 May 2014

Available online 4 June 2014

Keywords:

G-quadruplex DNA

Cisplatin

Fluorescence biosensor

Urine

ABSTRACT

Cisplatin is a widely used anticancer chemotherapeutic, and fast, convenient detection methods for it are highly desirable. Based on the interaction of cisplatin with G-quadruplex DNA, we developed a simple label-free fluorescence method for rapid cisplatin detection. The titration experiment showed that the cisplatin concentration and the fluorescence signal change ratios (F_0/F) exhibited a consistent linear correlation within the 1 to 10 μM range with a limit of detection of 720 nM, which was even lower than the common concentration of cisplatin in chemotherapy patients' urine (54.3 to 321 μM). The equilibrium dissociation constant K_D value for cisplatin binding was determined to be 1.19×10^{-5} M. This result demonstrated that our method had relatively high affinity toward cisplatin and could bind micromolar concentrations of cisplatin in solution. Our method also shows obvious selectivity among tested drugs, even between cisplatin and oxaliplatin/carboplatin. We demonstrated the high sensitivity of this methodology in the direct detection of cisplatin in urine samples and the fluorescence imaging of cisplatin in living cells.

© 2014 Elsevier B.V. All rights reserved.

1. Introduction

Since it was approved by the Food and Drug Administration (FDA) in 1978, cisplatin [*cis*-diamminedichloroplatinum(II)] has been widely used for treating solid tumors, such as germ cell tumors, carcinomas of the head and neck and other tumor types [1–4]. However, cisplatin administration has frequently shown toxic side effects, including nephrotoxicity, neurotoxicity and the induction of nausea and vomiting [5–7]. Furthermore, a low concentration (8 μM) of cisplatin led to cell apoptosis, while a high concentration (800 μM) resulted in necrotic cell death [8]. Thus, the dosage control of cisplatin is a key factor in the successful execution of cisplatin-based chemotherapy [8,9]. Previous reports suggested that the concentration of cisplatin varied from 54.3 to 321 μM in

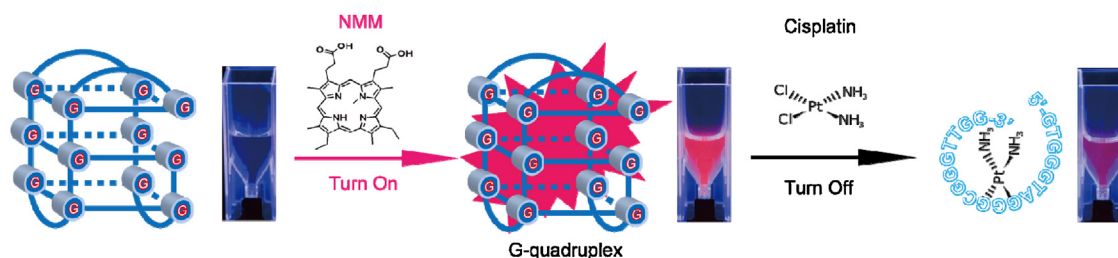
the urine of patients when administered at 50 mg/m^2 by slow injection [10,11], while 90% of excreted cisplatin remained unchanged chemically [9]. Therefore, methods to monitor either extracellular or intracellular cisplatin concentrations are highly desired to ensure effective chemotherapy.

Currently, a series of analytical methods have been developed for measuring cisplatin [12]. The traditional methods utilising optical detection of cisplatin in biological samples required a complicated derivatization processes [9,10]. Recently, Petrlova et al. [13] and Mascini et al. [14] designed several powerful electrochemical biosensors for detecting cisplatin in solution. However, these biosensors encountered complications with cisplatin enrichment on the electrode surface [15]. Techniques such as atomic absorption spectrometry (AAS) [16] and inductively coupled plasma-mass spectrometry (ICP-MS) [17] could be used in analyzing the platinum content from cisplatin following complicated sample preparation processes. Thus, a fast, convenient and low-cost method with high cisplatin detection sensitivity in biological samples will be highly advantageous.

Herein, we report a simple method to detect cisplatin by utilising the interaction between cisplatin and G-quadruplex DNA. G-quadruplex DNA, a certain type of G-rich nucleic acid sequence

* Corresponding authors at: State Key Laboratory of Pharmaceutical Biotechnology, Institute of Chemistry and BioMedical Sciences, School of Life Sciences, Nanjing University, 22 Hankou Road, Nanjing, Jiangsu, China.
Tel.: +86 025 84687371/+86 136 75149425.

E-mail addresses: yanghualin2005@126.com (H. Yang), jingzhao@nju.edu.cn (J. Zhao).



Scheme 1. Schematic illustration of the label-free fluorescence DNA probe based on the cisplatin-induced allosteric G-quadruplex for the detection of cisplatin.

[18,19], plays an important role in genomic functions, including transcription, recombination and replication [20–23]. Interestingly, unlike triplex, duplex or single-stranded forms of DNA, G-quadruplex DNA can be selectively recognized by N-methyl mesoporphyrin IX (NMM) [24,25]. The fluorescence intensity of NMM exhibits a dramatic enhancement upon binding to G-quadruplex DNA [26,27]. Recent research progress has shown that this interaction can be utilized as a signal reporter to detect heavy metal ions [28], NAD⁺ [29] and RNA [30,31]. Furthermore, it was reported that cisplatin hydrolysed to produce cationic species after passing through the blood into the cells. The platinum atoms of the cationic species would subsequently covalently bond to the nitrogen atoms of guanine on the basic backbone of the DNA, forming intra- and inter-strand crosslink [32] that result in structural destruction of the target DNA [33]. Inspired by these reports, we proposed that an easy, highly sensitive method of cisplatin detection could be developed by adding cisplatin to the combination of G-quadruplex DNA and NMM. As shown in Scheme 1, the self-folding of G-quadruplex DNA without cisplatin would form a G-quadruplex DNA structure that binds NMM and results in a remarkable hyperchromic effect. When cisplatin was added, it would bind to G-quadruplex DNA and disintegrate the DNA structure of the G-quadruplex, which would result in an obvious hypochromic effect.

2. Experimental

2.1. Chemicals and materials

The synthetic G-rich oligonucleotides DNA purified by PAGE were obtained from Shanghai Sangon Biological Engineering Technology & Services Co., Ltd. (Shanghai, China). Stock solution of G-rich oligonucleotides (100 μM) was prepared by DNase- and RNase-free water. Before used, the oligonucleotides solutions were diluted to required concentration with the Tris–HCl buffer (10 mM, pH 7.6). Cisplatin and NMM were purchased from J&K Scientific Ltd. (Beijing, China). Other anti-cancer drugs were purchased from Sigma-Aldrich. All chemicals were analytical reagent. The water used was purified by Millipore Milli-Q (18 M Ω/cm). The stock solution of NMM (6 mM) was prepared in DMSO [dimethyl sulfoxide], stored in darkness at –20 °C. Before being used, NMM was diluted to required concentration with the Tris–HCl buffer (10 mM, pH 7.6).

2.2. Fluorometric analysis

All fluorescence measurements were performed on an F-7000 spectrometer (Hitachi, Japan). The instrument settings were as follows: Excitation wavelength λ_{EX} = 399 nm (bandpass 10 nm), Emission wavelength λ_{EM} from 550 nm to 700 nm (bandpass 10 nm) and the photomultiplier tube (PMT) detector voltage = 500 V. The cisplatin titration was performed by adding 1 μM to 100 μM cisplatin into 125 nM PS2.M oligonucleotide DNA in Tris–HCl buffer (10 mM, pH 7.6) containing 2 mM KCl and 1.5 μM NMM. All samples

were incubated at 37 °C for 80 min to ensure completed reaction and signal stabilization. The fluorescence signal change ratios were calculated with the formula $Y = F_0/F$, where F_0 and F are the fluorescence intensities at 610 nm (maximum emission wavelength) in the absence and presence of cisplatin, respectively.

2.3. Circular dichroism (CD) spectra measurement

The G-quadruplex oligonucleotides (30 μM) were dissolved in 10 mM potassium acetate. The CD spectra were measured using a JASCO J-810 CD spectropolarimeter (Jasco, Japan). The data were recorded for the 220 to 320 nm range at room temperature in a quartz cuvette with a 1 mm optical path length. The data reported herein were averaged from at least 5 scans to improve the signal-to-noise ratio so that the contribution from the buffer was diminished.

2.4. Rat urine experiments

SD rats (8 weeks old) were purchased from Model Animal Research Center of Nanjing University. The rats were provided with a standard pelleted food and water and were placed in metabolism cages. Rats treated with 10 mg/kg cisplatin by intraperitoneal injection and treated with the same volume of normal saline as a control. The urine was collected for 24 h and stored frozen until analysed. Before measured, the urine samples were centrifuged and filtered by a 0.22 μm filter. The animal study proposal was approved by the Institutional Animal Care and Use Committee (IACUC) of the Nanjing University. All rat experimental procedures were performed in accordance with the Regulations for the Administration of Affairs Concerning Experimental Animals approved by the State Council of People's Republic of China. An experiment of normal urine samples with extra added cisplatin was also conducted by the same method.

2.5. Cellular imaging experiments

Human breast adenocarcinoma (MCF-7) cells were cultured in Dulbecco's modified Eagle's medium (DMEM) supplemented with 10% foetal bovine serum (FBS) in an atmosphere of 5% CO₂ and 95% air at 37 °C. The cells were allowed to grow to 80% confluency before being transfected. At that time, oligonucleotide transfections were performed using 500 nM G-quadruplex DNA, 6 μM NMM, 2 mM K⁺ and Lipofectamine 2000 reagent (Invitrogen). One hour after transfection, the media was removed and fresh media was added to remove any material left in solution and to optimize the background signal. For the cisplatin treatment, the cells were incubated with 10 μM cisplatin for 12 h. The Hoechst 33342 was added 20 min before the imaging experiments. All imaging experiments were performed using a confocal microscope (Olympus FV 1000). Both NMM and Hoechst 33342 used the DAPI filter and their excitation wavelengths were both set at 387 nm; however, their emission wavelengths were 610 nm and 440 nm, respectively.

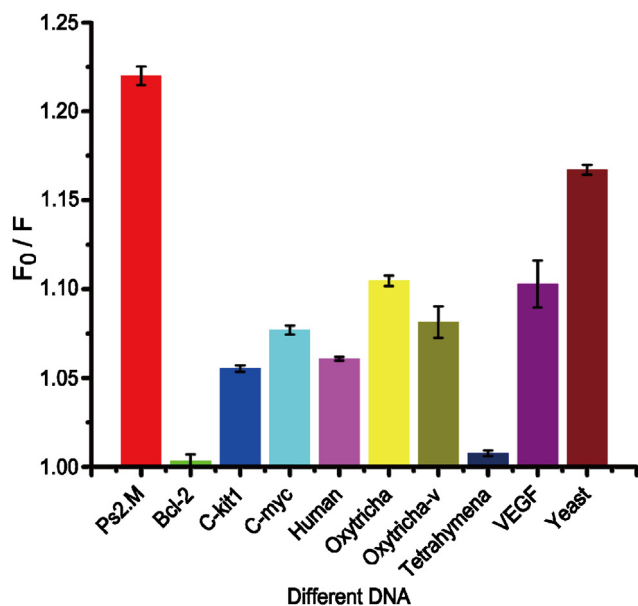


Fig. 1. G-rich oligonucleotides were screened for fluorescence signal change ratios (F_0/F). 125 nM different G-quadruplex DNA was incubated with 10 μM NMM and 10 mM K^+ in Tris–HCl buffer (10 mM, pH 7.6) in the presence of 5 μM cisplatin. Excitation: 399 nm, emission: 610 nm. The data represent the mean \pm SD of at least three independent experiments. F_0 and F are the fluorescence intensities in the absence and presence of cisplatin, respectively.

3. Results and discussion

3.1. Optimization

Ten kinds of G-quadruplex DNA sequences (see Table S1 in Supporting information) were initially screened. PS2.M, isolated from an artificial library of random DNA sequences [34,35], was selected because of its high level of fluorescence intensity (see Fig. S1 in Supporting information) and high fluorescence signal change ratios (F_0/F) at 610 nm (Fig. 1). Besides, the concentration of G-quadruplex stabilizing K^+ (see Fig. S2 in Supporting information) and NMM (see Fig. S3 in Supporting information) were optimized to guarantee better effect of measurement.

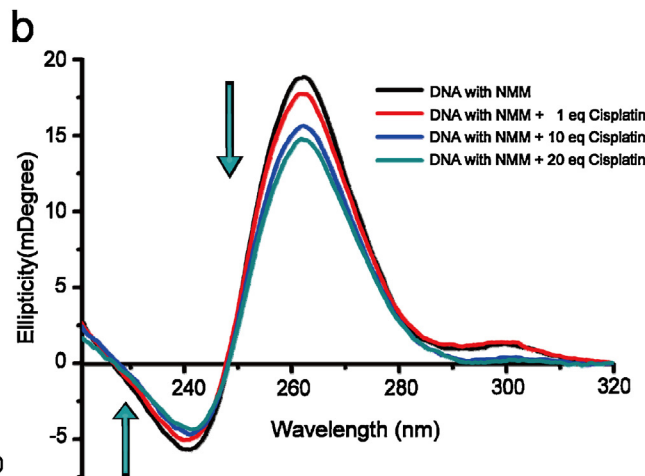
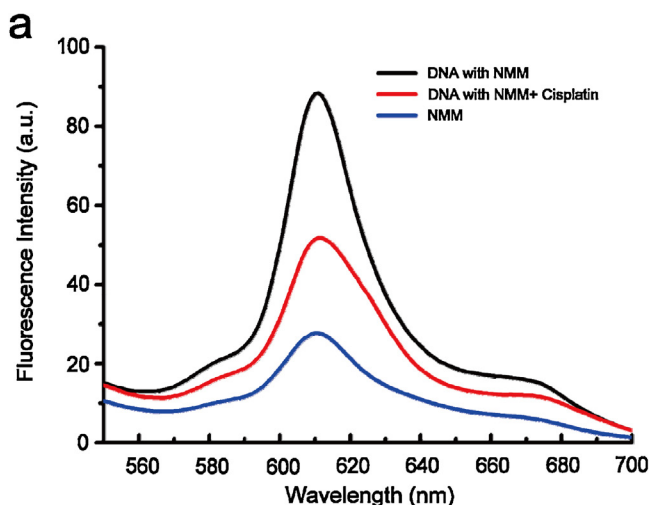


Fig. 2. (a) The fluorescence spectrum of 1.5 μM NMM and 125 nM DNA in 2.0 mM K^+ and 10 mM Tris–HCl (pH 7.6) buffer (black curve) and the spectrum after the addition of 10 μM cisplatin (red curve). The sample containing only 1.5 μM NMM in buffer (blue curve) was the control. Excitation: 399 nm, emission: 550–700 nm. (b) The CD spectra of 30 μM G-quadruplex DNA with 30 μM NMM in the presence of various molar equivalents of cisplatin. The G-quadruplex DNA displayed a characteristic elliptical peak at 262 nm and a trough at 240 nm. (For interpretation of the references to color in this figure legend, the reader is referred to the web version of this article.)

3.2. Feasibility

To confirm the feasibility of the present strategy, the fluorescence emission spectra from 550 to 700 nm under different conditions were investigated when the compounds were excited at 399 nm in 10 mM Tris–HCl buffer (pH 7.6) (Fig. 2a). NMM showed very faint fluorescence by itself (Fig. 2a, blue) but exhibited a dramatic enhancement upon the addition of 125 nM G-quadruplex DNA (PS2.M) (Fig. 2a, black). After the subsequent addition of 10 μM cisplatin, the fluorescence emission significantly decreased by 41.74% (from 88.24 to 51.41 of the relative fluorescence intensity) within 80 min to ensure completed reaction and signal stabilization (Fig. 2a, red; see Fig. S4 in Supporting information).

Additionally, to probe the mechanism of the fluorescence change, the circular dichroism (CD) spectra of G-quadruplex DNA samples were measured at various cisplatin concentrations. As shown in Fig. 2b, in the absence of cisplatin, the G-quadruplex DNA showed a characteristic elliptical peak of 18.54 mdeg at 262 nm and a trough of -5.93 mdeg at 240 nm. However, the values at the peak and the trough decreased gradually with an increase in cisplatin concentration. When 20 equivalents of cisplatin were added, the elliptical peak decreased by 21.04% to 14.64 mdeg and the trough increased by 26.98% to -4.33 mdeg. The MS (see Fig. S5 in Supporting information) and electrophoresis study (see Fig. S6 in Supporting information) were also conducted to confirm the binding between cisplatin and PS2.M. The results showed that this PS2.M DNA could bind to two cisplatin molecules. Thus, the decrease in fluorescence correlated with the conformational change of G-quadruplex DNA following the addition of cisplatin.

3.3. Sensitivity

Subsequently, varying concentrations of cisplatin (1–100 μM) were added to the experimental system to test the detection range of this sensing strategy. The fluorescence intensity decreased with cisplatin concentrations up to 100 μM (Fig. 3a). This result indicated that the structural distortion of the G-quadruplex DNA was highly associated with the concentration of cisplatin. The fluorescence signal change ratios (F_0/F) at 610 nm in the presence of varying cisplatin concentrations were observed. When the cisplatin concentration was within the 1 to 100 μM range, the calibration curve showed a sigmoidal shape and matched the dose–response curve

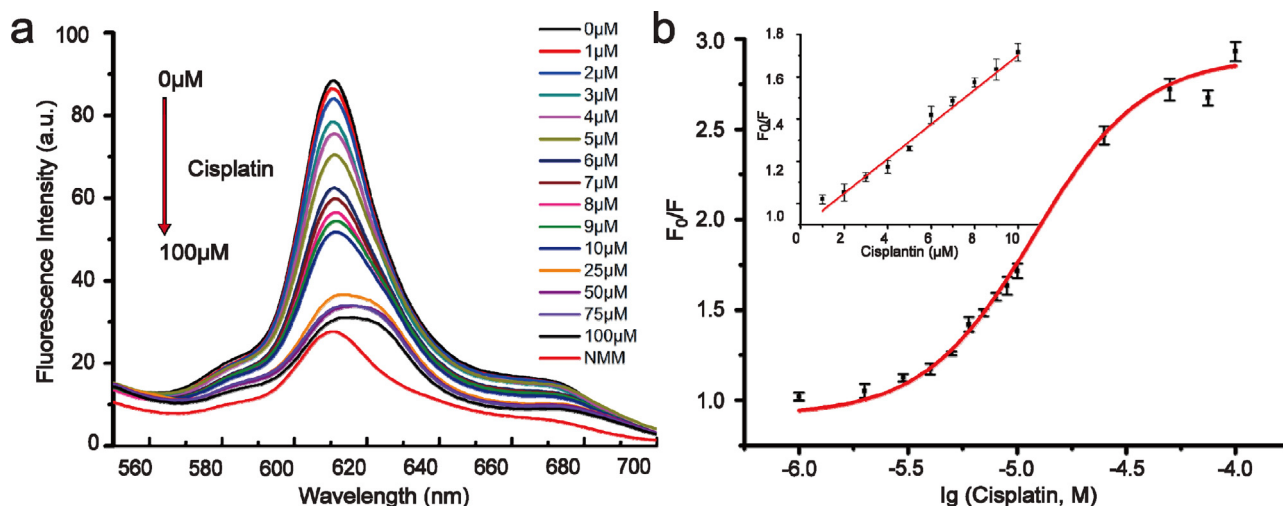


Fig. 3. (a) The fluorescence spectra of 10 mM Tris–HCl (pH 7.6) containing 1.5 μM NMM, 125 nM DNA and 2.0 mM K^+ in the presence of increasing cisplatin concentrations. (b) The fluorescence signal change ratios (F_0/F) at 610 nm for cisplatin concentrations ranging from 1 to 100 μM , which matched the dose–response curve. Inset: the fluorescence signal ratios at low (1–10 μM) cisplatin concentrations (matching a linear relationship). F_0 and F are the fluorescence intensities in the absence and presence of cisplatin, respectively. Error bars were estimated from at least three independent measurements.

dependence of F_0/F on the logarithm (\lg) of cisplatin concentration ($R^2 = 0.994$) (Fig. 3b). The equilibrium dissociation constant K_D value for cisplatin binding was determined to be 1.19×10^{-5} M on the basis of the fitting of the curve. This result demonstrated that PS2.M had relatively high affinity toward cisplatin and could bind micromolar concentrations of cisplatin in solution. The fluorescence signal change ratio (F_0/F) increased proportionally with concentrations of cisplatin within the 1 to 10 μM range ($R^2 = 0.985$) (inset in Fig. 3b). The limit of detection for cisplatin was estimated to be 720 nM, which was better than or comparable to the values obtained by other methods (see Table S2 in Supporting information). Furthermore, our method can directly detect the cisplatin instead of platinum atoms. Therefore, we can calculate the concentration of cisplatin according to the linear correlation between cisplatin and the fluorescence signal change ratios (F_0/F).

3.4. Selectivity

Additionally, the selectivity of our method was later evaluated by comparing the fluorescence signal change ratios (F_0/F) in the presence of individual anticancer drugs that have similar DNA–interaction mechanisms. As shown in Fig. 4, the concentrations of all of the tested anticancer drugs including cisplatin were all 20 μM , but only the cisplatin test resulted in a considerably large fluorescence emission ratio. When compared to other anticancer drugs, our method demonstrated peak selectivity for cisplatin with a F_0/F of 3.10, while other compounds remained below 1.23 with the exception of oxaliplatin (1.69) which was still a significant difference, even in the high concentrations (see Fig. S7 in Supporting information). The ratio disparity between other anticancer compounds and cisplatin indicated high selectivity of our method for cisplatin. Because the reaction mechanisms of oxaliplatin and carboplatin are relatively similar to that of cisplatin [36,37], the interferences between them were also examined. The ratiometric signals of the reaction of G–quadruplex DNA with these platinum drugs at 10 μM concentrations were thus measured before and after the addition of an equal amount of 10 μM cisplatin. According to the data, the F_0/F ratios of carboplatin was nearly indistinguishable from the control (1.00), and that of oxaliplatin was also low at 1.28, both being much lower than cisplatin (1.91). However, the ratios all rose to 1.91 soon after the addition of cisplatin, showing

that the presence of oxaliplatin and carboplatin did not affect the cisplatin testing results in our assay conditions (inset in Fig. 4). The result was consistent with other reported electrochemical method based on the reactivity of guanine and compounds (cisplatin, carboplatin, $[\text{Pt}(\text{bpy})(\text{py})_2]^{2+}$, etc.) [14]. The excellent selectivity among all tested drugs could be due to the poly guanine DNA sequence and the high binding affinity between cisplatin and guanine *via* the robust covalently bond, while the selectivity among platinum compounds could be attribute to a substantially higher reaction rate for Pt–DNA formation caused by cisplatin compared with oxaliplatin [38] and carboplatin [14].

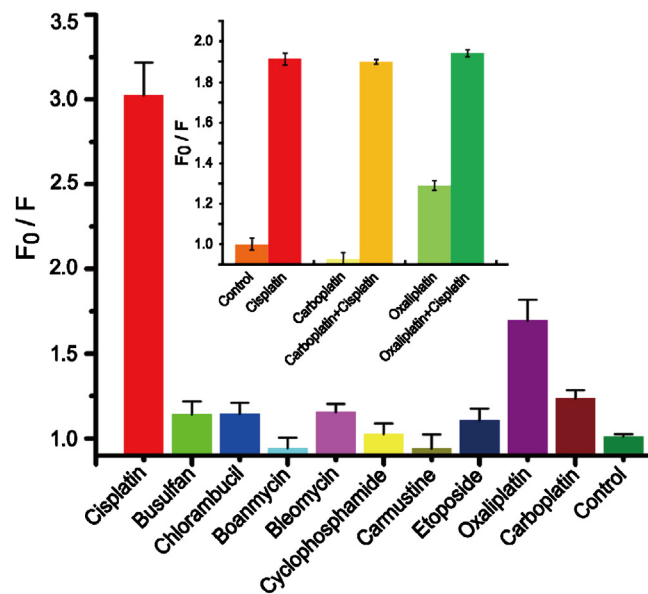


Fig. 4. The selectivity of our system for cisplatin compared with other anticancer drugs illustrated by the measured fluorescence signal change ratios (F_0/F) in the presence of various 20 μM anticancer drugs. The control was a sample assayed without the addition of any anticancer drugs. Inset: The interference study of our system that investigated the fluorescence signal change ratios (F_0/F) in the presence of several 10 μM platinum compounds as well as the co-administration of these compounds with 10 μM cisplatin. The data represent the mean \pm SD of at least three independent experiments.

Table 1
Measurement of metabolic cisplatin concentrations in urine.

Sample	ICP-AES (μM)	Our method (μM)	P-values (<i>t</i> -test)
1	104.2	103.7 \pm 15.1	0.48 > 0.05
2	99.9	100.1 \pm 10.5	0.49 > 0.05
3	128.3	117.6 \pm 9.9	0.10 > 0.05
4	98.9	96.6 \pm 13.12	0.39 > 0.05

3.5. Determination of cisplatin in urine

With the ideal sensitivity and selectivity established in a reaction solution, our method was further applied to test urine samples collected from rats. Previous reports had suggested that the concentration of cisplatin varied from 54.3 to 321 μM in the urine of patients [9,10]. Considering the high sensitivity of our method, the urine samples were 50 times diluted before measurements. Through the equation of standard curve, we could get the back-calculated concentration of cisplatin. As shown in Table 1, our method showed excellent agreement with inductively coupled plasma atomic emission spectroscopy (ICP-AES). The recovery was

Table 2
Measurement of added cisplatin concentrations in urine.

Sample	Added cisplatin (μM)	Our method (μM)	Recovery (%)
1	100	101.44 \pm 4.92	101.44
2	100	96.36 \pm 6.12	96.36
3	100	97.75 \pm 4.21	97.75
4	100	106.21 \pm 7.01	106.21

also tested and found to be in the range of 96.36–106.21% (Table 2). These results indicated that this proposed method could be used in urine samples.

3.6. Cellular imaging experiments

The ability of our method to track cisplatin in living cells was also assessed. After the transfection of G-quadruplex DNA and NMM into MCF-7 tumor cells, bright red fluorescence was shown in living cells (Fig. 5a). After 12 h, upon the addition of 10 μM cisplatin, a significant decrease in fluorescence intensity was observed in the cytoplasm (Fig. 5e). Much weaker fluorescence was observed

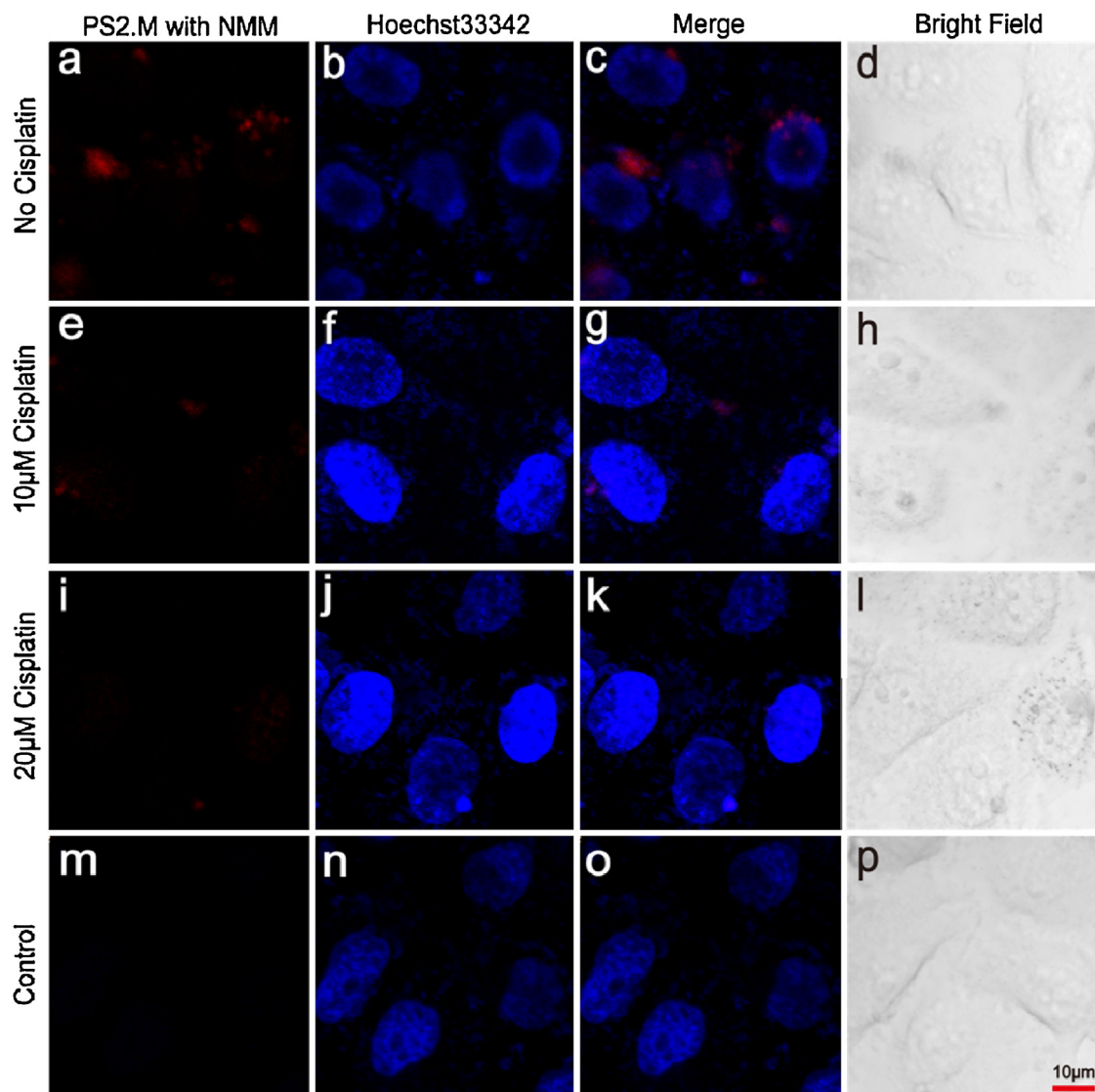


Fig. 5. Live-cell imaging of cisplatin by confocal microscopy. ((a)–(d)) Imaging of MCF-7 cells incubated with G-quadruplex DNA and NMM without cisplatin. Cells were co-stained with Hoechst 33342 to show the cell nuclei. Single confocal image planes of NMM emitted red and Hoechst 33342 emitted blue. The merged groups are the red and blue channels overlaid together. ((e)–(h)) Imaging of fluorescence decrease in cells with 10 μM cisplatin. ((i)–(l)) Imaging of fluorescence decrease in cells with 20 μM cisplatin. ((m)–(p)) The control groups, which did not have added G-quadruplex DNA and cisplatin. The scale bar represents 10 μm .

if 20 μ M cisplatin was added (Fig. 5i). Although not quantitative in living cell at present, these imaging results still suggest that our method could potentially be a tool for probing the response to cisplatin in live-cell imaging.

4. Conclusions

In summary, a novel fluorescence method for convenient and highly sensitive detecting cisplatin based on the conformational interactions between NMM and G-quadruplex DNA was developed and explored while there are few reports on fluorescent methods without complicated derivatization processes. Our method also shows obvious selectivity among tested drugs, even between cisplatin and oxaliplatin/carboplatin. Furthermore, it is not interfered by biological autofluorescence [39,40] owing to the emission wavelength of NMM (610 nm). Meanwhile, the lasting fluorescence allows an overnight measurement (see Fig. S8 in Supporting information). This sensitive and selective fluorescent method has the potential to be a useful tool for detecting cisplatin in mouse urine and can be used for imaging cisplatin in live cells.

Acknowledgments

This work is financially supported by grants from the National Basic Research Program of China (2010CB923303), the National High Technology Research and Development Program of China (2014AA020512), and the Jiangsu Natural Science Foundation (BK2011547). J. Z. thanks the National Natural Science Foundation of China (91013009), Guangdong Government (S20120011226), and the Shenzhen Government (JC201104210113A KQC201105310016A) for support. W. W. thanks the National Natural Science Foundation of China (31200607).

Appendix A. Supplementary data

Supplementary data associated with this article can be found, in the online version, at <http://dx.doi.org/10.1016/j.snb.2014.05.027>.

References

- [1] D. Wang, S.J. Lippard, Cellular processing of platinum anticancer drugs, *Nat. Rev. Drug Discovery* 4 (2005) 307–320.
- [2] B. Rosenberg, L. VanCamp, J.E. Trosko, V.H. Mansour, Platinum compounds: a new class of potent antitumor agents, *Nature* 222 (1969) 385–386.
- [3] R.B. Weiss, M.C. Christian, New cisplatin analogues in development, *Drugs* 46 (1993) 360–377.
- [4] R.C. Young, D.D. Von Hoff, P. Gormley, R. Makuch, J. Cassidy, D. Howser, J.M. Bull, *cis*-Dichlorodiammineplatinum(II) for the treatment of advanced ovarian cancer, *Cancer Treat. Rep.* 63 (1979) 1539–1544.
- [5] J.M. Hill, R.J. Speer, Organo-platinum complexes as antitumor agents (review), *Anticancer Res.* 2 (1982) 173–186.
- [6] B. Rosenberg, Noble metal complexes in cancer chemotherapy, *Adv. Exp. Med. Biol.* 91 (1977) 129–150.
- [7] N.E. Madias, J.T. Harrington, Platinum nephrotoxicity, *Am. J. Med.* 65 (1978) 307–314.
- [8] A.H. Lau, Apoptosis induced by cisplatin nephrotoxic injury, *Kidney Int.* 56 (1999) 1295–1298.
- [9] K.Y. Inagaki, S.Y. Kidani, Direct determination of *cis*-dichlorodiammineplatinum(II) in urine by derivative spectroscopy, *Chem. Pharm. Bull.* 33 (1985) 3369–3374.
- [10] B. Anilnert, G. Yalçin, F. Ariöz, E. Dölen, The spectrophotometric determination of cisplatin in urine, using *o*-phenylenediamine as derivatizing agent, *Anal. Lett.* 34 (2001) 113–123.
- [11] C.M. Riley, L.A. Sternson, A.J. Repta, R.W. Siegler, High-performance liquid chromatography of platinum complexes on solvent generated anion exchangers. III. Application to the analysis of cisplatin in urine using automated column switching, *J. Chromatogr.* 229 (1982) 373–386.
- [12] M.E. Bosch, A.J. Sanchez, F.S. Rojas, C.B. Ojeda, Analytical methodologies for the determination of cisplatin, *J. Pharm. Biomed. Anal.* 47 (2008) 451–459.
- [13] J. Petrlova, D. Potesil, J. Zehnalek, B. Sures, V. Adam, L. Trnkova, R. Kizek, Cisplatin electrochemical biosensor, *Electrochim. Acta* 51 (2006) 5169–5173.

- [14] M. Mascini, G. Bagni, M.L. Di Pietro, M. Ravera, S. Baracco, D. Osella, Electrochemical biosensor evaluation of the interaction between DNA and metallo-drugs, *Biometals* 19 (2006) 409–418.
- [15] P. Shearan, M.R. Smyth, Comparison of voltammetric and graphite furnace atomic absorption spectrometric methods for the direct determination of inorganic platinum in urine, *Analyst* 113 (1988) 609–612.
- [16] M. Verschraagen, K. van der Born, T.H. Zwiers, W.J. van der Vijgh, Simultaneous determination of intact cisplatin and its metabolite monohydrated cisplatin in human plasma, *J. Chromatogr. B: Analyt. Technol. Biomed. Life Sci.* 772 (2002) 273–281.
- [17] D.N. Bell, J.J. Liu, M.D. Tingle, M.J. McKeage, Specific determination of intact cisplatin and monohydrated cisplatin in human plasma and culture medium ultrafiltrates using HPLC on-line with inductively coupled plasma mass spectrometry, *J. Chromatogr. B: Analyt. Technol. Biomed. Life Sci.* 837 (2006) 29–34.
- [18] D. Sen, W. Gilbert, Formation of parallel four-stranded complexes by guanine-rich motifs in DNA and its implications for meiosis, *Nature* 334 (1988) 364–366.
- [19] H. Han, L.H. Hurley, G-quadruplex DNA: a potential target for anti-cancer drug design, *Trends Pharmacol. Sci.* 21 (2000) 136–142.
- [20] I. Cheung, M. Schertzer, A. Rose, P.M. Lansdorf, Disruption of dog-1 in *Caenorhabditis elegans* triggers deletions upstream of guanine-rich DNA, *Nat. Genet.* 31 (2002) 405–409.
- [21] A. Siddiqui-Jain, C.L. Grand, D.J. Bearss, L.H. Hurley, Direct evidence for a G-quadruplex in a promoter region and its targeting with a small molecule to repress c-MYC transcription, *Proc. Nat. Acad. Sci. U.S.A.* 99 (2002) 11593–11598.
- [22] A.K. Todd, M. Johnston, S. Neidle, Highly prevalent putative quadruplex sequence motifs in human DNA, *Nucleic Acids Res.* 33 (2005) 2901–2907.
- [23] E.Y. Lam, D. Beraldi, D. Tannahill, S. Balasubramanian, G-quadruplex structures are stable and detectable in human genomic DNA, *Nat. Commun.* 4 (2013) 1796.
- [24] J.M. Nicoludis, S.T. Miller, P.D. Jeffrey, S.P. Barrett, P.R. Rablen, T.J. Lawton, L.A. Yatsunyk, Optimized end-stacking provides specificity of N-methyl mesoporphyrin IX for human telomeric G-quadruplex DNA, *J. Am. Chem. Soc.* 134 (2012) 20446–20456.
- [25] J.M. Nicoludis, S.P. Barrett, J.L. Mergny, L.A. Yatsunyk, Interaction of human telomeric DNA with N-methyl mesoporphyrin IX, *Nucleic Acids Res.* 40 (2012) 5432–5447.
- [26] H. Arthanari, S. Basu, T.L. Kawano, P.H. Bolton, Fluorescent dyes specific for quadruplex DNA, *Nucleic Acids Res.* 26 (1998) 3724–3728.
- [27] S.S. Oh, K. Plakos, X. Lou, Y. Xiao, H.T. Soh, In vitro selection of structure-switching, self-reporting aptamers, *Proc. Nat. Acad. Sci. U.S.A.* 107 (2010) 14053–14058.
- [28] L. Guo, D. Nie, C. Qiu, Q. Zheng, H. Wu, P. Ye, Y. Hao, F. Fu, G. Chen, A G-quadruplex based label-free fluorescent biosensor for lead ion, *Biosens. Bioelectron.* 35 (2012) 123–127.
- [29] J. Zhao, L. Zhang, J. Jiang, G. Shen, R. Yu, A label-free fluorescence DNA probe based on ligation reaction with quadruplex formation for highly sensitive and selective detection of nicotinamide adenine dinucleotide, *Chem. Commun. (Camb)* 48 (2012) 4468–4470.
- [30] B.C. Yin, Y.Q. Liu, B.C. Ye, One-step, multiplexed fluorescence detection of microRNAs based on duplex-specific nuclease signal amplification, *J. Am. Chem. Soc.* 134 (2012) 5064–5067.
- [31] D.L. Ma, H.Z. He, K.H. Leung, H.J. Zhong, D.S. Chan, C.H. Leung, Label-free luminescent oligonucleotide-based probes, *Chem. Soc. Rev.* 42 (2013) 3427–3440.
- [32] S.F. Bellon, J.H. Coleman, S.J. Lippard, DNA unwinding produced by site-specific intrastrand cross-links of the antitumor drug *cis*-diamminedichloroplatinum(II), *Biochemistry* 30 (1991) 8026–8035.
- [33] C. Demarcq, R.T. Bunch, D. Creswell, A. Eastman, The role of cell cycle progression in cisplatin-induced apoptosis in Chinese hamster ovary cells, *Cell Growth Differ.* 5 (1994) 983–993.
- [34] P. Travascio, Y. Li, D. Sen, DNA-enhanced peroxidase activity of a DNA-aptamer-hemin complex, *Chem. Biol.* 5 (1998) 505–517.
- [35] Y. Li, C.R. Geyer, D. Sen, Recognition of anionic porphyrins by DNA aptamers, *Biochemistry* 35 (1996) 6911–6922.
- [36] E. Raymond, S.G. Chaney, A. Taamma, E. Cvitkovic, Oxaliplatin: a review of preclinical and clinical studies, *Ann. Oncol.* 9 (1998) 1053–1071.
- [37] F.A. Blommaert, H.C. van Dijk-Knijnenburg, F.J. Dijt, L. den Engelse, R.A. Baan, F. Berends, A.M. Fichtinger-Schepman, Formation of DNA adducts by the anticancer drug carboplatin: different nucleotide sequence preferences in vitro and in cells, *Biochemistry* 34 (1995) 8474–8480.
- [38] C.P. Saris, P.J. van de Vaart, R.C. Rietbroek, F.A. Blommaert, In vitro formation of DNA adducts by cisplatin, lobaplatin and oxaliplatin in calf thymus DNA in solution and in cultured human cells, *Carcinogenesis* 17 (1996) 2763–2769.
- [39] J.E. Aubin, Autofluorescence of viable cultured mammalian cells, *J. Histochem. Cytochem.* 27 (1979) 36–43.
- [40] H. Andersson, T. Baechi, M. Hoechl, C. Richter, Autofluorescence of living cells, *J. Microsc.* 191 (1998) 1–7.

Biographies

Hualin Yang received his B.S. from Liaocheng University in 2008. He is now a Ph.D. candidate in School of Life Sciences, Nanjing University. His current interests are biosensors.

Hanli Cui received his B.S. from Henan University of Science and Technology in 2011. Now he is a MS candidate in School of Life Sciences, Nanjing University. His research work is focused on the structure and function of large biological molecules.

Longgang Wang received his B.S. from Dezhou University in 2010. He is now a MS candidate in School of Life Sciences, Nanjing University. His current interest is the development of yeast surface display system.

Li Yan received her B.S. from Agricultural University of Hebei in 2010. She is now a PhD candidate in School of Life Sciences, Nanjing University. Her current interests are RNA detection by fluorescence methods.

Yong Qian received his Ph.D. from Nanjing University in 2012. He is currently an assistant professor at Nanjing University, China. His research interests are focusing

on the design and application of fluorescent probes and the research of pharmacological active compounds for the treatment of cancer.

Xi Emily Zheng received her Ph.D. from University of Washington in 2010. She is a preventive medicine fellow at Weill Cornell Medical College. Her current interests are clinical research and cancer therapy.

Wei Wei received his Ph.D. from Nanjing Normal University in 2010. He is currently an assistant professor at Nanjing University, China. His research interests are focusing on using microorganism to detect and adsorb heavy metal ions.

Jing Zhao received his Ph.D. from Yale University in 2005. He is currently a professor of Nanjing University and Peking University at Shenzhen, China. Now his research interests include the synthesis of small molecules with biological activities and the development of fluorescent probes.